Tuijin Jishu/Journal of Propulsion Technology
ISSN: 1001-4055
Vol. 44 No. 6 (2023)

Deep Learning Based Micro-Mechanical Model for Study of Thermo-Mechanical Behavior of Al-SiC MMC During FSW Process

[1]T. Madhavi, [2]D. V. Ravi Shankar, [3]K. Prasanna Lakshmi

*[1]Research Scholar, Department of Mechanical Engineering, Jawaharlal Nehru Technological University, Hyderabad, India *Corresponding Author,*

[2]Professor, Department of Mechanical Engineering, TKR College of Engineering and Technology, Meerpet, Hyderabad, India.

[3]Professor, Department of Mechanical Engineering, Jawaharlal Nehru Technological University, Hyderabad, India.

Abstract: Designing superior attributes using a combination of metals involves uncertainties and has lured the present interest since the early age of the evolution. In the current era, as numerous AI-based models are being developed and implemented in different engineering fronts, similar attempts are under process in metallurgy as a plethora of data has been annulled and is available for modern researchers to access and innovate techniques to be used to evaluate such materials. This paper aims to provide one such deep learning based micro-mechanical computational model to estimate thermo-mechanical behavior of Al-SiC Particulate Reinforced Metal Matrix Composites during Friction Stir Welding.

Keywords:*PRMMC,FSW,Deep learning,Micro Mechanical Model,Tensor Mechanics,*

LAMMPS

ε_0 : Strain

σ_0: uniform stress N/m2

Em : tensor of elastic modulus N/m^2

σ_V : average stress across volume N/m^2

ε_v: strain due to σ_v

P_{Vf} : particle volume fraction

$S_{P:}$: stiffness module of particle N/m^2

σ_P: particle stress N/m^2

ε_D: strain due to disturbance caused by σ_P

ε_+: average strain due to transformation

ET : Eshelby tensor m^2

ε_{total}: total volumetric strain

Γ : green's function

ε_a : average strain

$\varepsilon_{\Delta t}$ :: thermal induced eigen strain

d_p: diameter of particle. m

L_{vf} : liquid volume fraction,

ρ_L : density of liquid at given temperature kg/m^3

Re_p: Reynold's number of particle

μ_L : dynamic viscosity of Al at given temperature N/m s

V_∞ : called stokes settling velocity for a single particle.

ρ_P : particle density kg/m^3

τ : Jacobian matrix

1. Introduction

Recent years have witnessed an increase in research interest in Particulate Reinforced Metal Matrix Composites (PRMMC's) and their machining process. Their ability to handle sudden impacts has made them a valuable substitute for numerous marine, aerospace, and automotive applications. With such a potential for wide applicability, engineers and researchers are focused on improving their machining capabilities. Usually, such composites are made of softer matrix like aluminum reinforced by harder carbides of silicon or tungsten. The combination Al-SiC based matrices is mostly studied for it's easier to fabricate. Further, the feed-less welding techniques like Friction Stir Welding (FSW) are suggested to be apt for joining such material during fabrication.

The reliability of any modern engineering design is often first evaluated using a computational model. It is paramount to understand the upper and lower limits of its properties before employing them in real-world applications. The presence of binary metals without chemical bonding in such matrix-particle combinations presents a unique problem while implementing conventional finite element techniques. This has laid the foundation for micro-mechanical models studying the molecular dynamics of these materials using representative unit volume elements. This gets further complicated while studying nonlinear attributes such as stress induced friction or temperature induced strain. Such studies often call for more complex methods demanding higher computational resources.

Addition of particles helps to improve the resistance towards crack and increase the fracture toughness of matrix materials [1]. These particles are generally in micro and nano size. If the particle is of micro size, it is observed that size of particle and its volume fraction contribute towards affecting the mechanical properties of composite matrix [2]. In matrix composites with softer matrix and harder particles or vice versa at this particle scale, if volume fraction is to be fixedly maintained and size of particle is to be decreased, then the strength of material is found to increase and the increment is reversed if particle size is constant and volume fraction is to increased [3].whereas the effective moduli are found to be more dependent on volume fraction rather than on size of particulates[4,5] Further in such composites, the strain during failure is less dependent on particle size and is significantly improved by surface treatment due to increase in interfacial adhesion[6]. In nano sized particulate additives, they prominently influence both strength and property moduli's of MMC's [7]. The thermo-rheological behavior and responses in visco-elastic state under high loading conditions of such reinforced MMC's is also dependent on particle size and distribution [8-11].The numerical in situ modeling of such matrix particle composites is often performed using two approaches primary. In case one, the existence of particulate is completely ignored and the MMC's are treated as single unit with continuous and constant stress-strain fields [12,13]. Where as in case two, the material is modelled as a homogenous distributed continuous mixture of matrix and particle[14,15]. A number of models have been presented to represent such homogenous composites, some of which are diluted distribution models, periodically distributed models and randomly distributed models [16-18].

With recent developments in data science, many have suggested a new generation of models driven by AI supported microstructure analysis of MMC's using X-rays or SEM images and using the collected data to train machine learning models to generate representative finite elements of such matrix-particle combinations [19-22].

2. Numarical modelling

2. 1.Mathematical Model for FSW process in PRMMCs

The FSW process in PRMMCs can be divided into two stages.

1. Strain induced due to temperature rise because of applied normal stress and frictional force.
2. Cohesive debonding of particulate from matrix followed by solidification of matrix around displaced particulate.

The first stage can be calculated using the following methodology.

The uniform stress σ_0 and induced uniform strains $\varepsilon_0$on an infinite elastic body is

$\varepsilon_0 = Em^{-1} \times \sigma_0$……………………….**(1)**[23]

where Em is tensor of elastic modulus.

In case of elliptical shaped inclusions in the matrix. The resultant stress is given by

$\sigma_n = \sigma_0 + \sigma_v = Em(\varepsilon_0 + \varepsilon_v)\ \sigma_0$……………………….**(2)**

where σ_V is average stress across volume. Similarly, $\varepsilon_v$is strain due to σ_v.

when integrated over total volume.

$Em\left[\varepsilon_v + P_{Vf}(\varepsilon_D - \varepsilon_+)\right] = 0$……………………….**(3)**

$\sigma_P = S_P\varepsilon_P = S_P(\ \varepsilon_V + \varepsilon_O + \varepsilon_D) = Em(\ \varepsilon_V + \varepsilon_O + \varepsilon_D - \varepsilon_+)$ ……………………….**(4)**

Where P_{Vf} is particle volume fraction,$S_P$is stiffness module of particle, $\sigma_P$is particle stress, $\varepsilon_D$is strain due to disturbance caused by σ_P,$\varepsilon_+$is average strain due to transformation.

$\varepsilon_D = ET.\varepsilon_+$……………………….**(5)**

Where ET is Eshelby tensor.

Further total volumetric strain can be written as

$\varepsilon_{total} = (I + mvB \times\ (I + mvC)^{-1} \times \varepsilon_0)$ ……………………….**(6)**

Where $\ B = AXT,\ A = I - Em^{-1} \times S_P,\ T = (I + ET \times Em^{-1} \times S_P - ET)^{-1}\ C = (ET - I) \times A \times T,$

I is identity matrix tensor

If the elastic modulus tensor of both Aland SIC are given by E_m^{Al} and E_m^{Sic} and overall thickness is T. If (x, y, z) denote global coordinate system then using Eshelby equivalent inclusion , the local strain field at certain point (x, y, z) for SIC embedded in Al under imposed normal stress and temperature change Δ_t.

$\varepsilon(x, y, z) =\ \varepsilon_0 +\ \varepsilon'(x, y, z)$ ……………………….**(7)**

Where $\varepsilon_0 = (E_m^{Sic})^{-1}{:}\ \sigma_0 + \alpha^{Sic}\Delta t\ \delta$

where ':' Is contraction between 4th and 2nd rank tensors , α^{Sic} is CTE, δ is Kronecker delta tensor[24,25]

$\varepsilon'(x, y, z) = \varepsilon_0(x, y, z) = \varepsilon_0(i) = \int_{I_0} \Gamma\left(i - i^l\right).(E_m^{Sic}){:}\ [\varepsilon_a\left(i^l\right) + \varepsilon_{\Delta t}]\ di^l$……………………….**(8)**

Where '.' is tensor contraction between two 4th rank tensor's.

Γ is green's function

ε_a is average strain and $\varepsilon_{\Delta t}$ is thermal induced Eigen strain ,$\varepsilon_{\Delta t}\ = (\alpha^{Al} - \alpha^{Sic})\Delta t\ \delta$

Tuijin Jishu/Journal of Propulsion Technology
ISSN: 1001-4055
Vol. 44 No. 6 (2023)

For sufficiently small RVE in infinite domain

$\Gamma(i - i') = \frac{1}{16\pi\mu^{Sic}(1-P_V^{sic})}[-\psi+(1+P_V^{sic})(\sum \delta\ \varphi)]$ ....**(9)**

Where $\psi = |i - i'|, \varphi = \frac{1}{|i-i'|}$

μ^{Sic}, P_V^{sic} are shear moduls and poison ratio matrices

$\Gamma(i - i')$ is response strain at i^{th} point due thermal eigen strain at i'^{th} point

The average eigen strain ε_a is derived as

$\varepsilon_a = (E_m^{Sic})^{-1}.(p^o - \Delta Em^{-1})^{-1}.(\varepsilon_a - \alpha^{Al}\Delta t\delta - p^o E_m^{Sic} : \varepsilon\Delta t)$ ....**(10)**

where $\Delta Em = E_m^{Al} - E_m^{Sic}$

$P_{mijkl}^0 = \frac{\delta_{ij}\delta_{ijkl}-(4-5P_V^{Sic})(\delta_{iK}\delta_{jL}+\delta_{il}\delta_{jk})}{30\mu^{Sic}(1-(P_V^{Sic})}$............................**(11)**

Thus local strain field is $\varepsilon_{local} = \alpha^{Al}\Delta t\delta + (I - p^6.\Delta Em)^{-1} : (\varepsilon_0 - \alpha^{Al}\Delta t\delta - p^0.E_m^{Sic} : \varepsilon_{\Delta t})$

whereI_{ijkl} is standard 4^{th} rank

$\frac{\delta_{iK}\delta_{jL}+\delta_{il}\delta_{jk}}{2} = \text{Unit tensor}$ ....**(12)**

When additional particles are introduced the interaction between them and i^{th} particle is given by

$< \varepsilon >^{Al}(0) = \alpha^{Al}\Delta t\delta + (I - p^o.\Delta Em)^{-1} : \left[< \varepsilon >^{sic}(0) - \alpha^{Al}\Delta t\delta - p^o.\Delta Em^{\ Sic} : E^{\Delta t}\right] + \sum_{L=1}^{\infty}(\Delta Em^{\ -1}.L(0,i)) : (\varepsilon_0 - \alpha^{Al}\Delta t\delta - \Delta Em^{\ -1}.Em^{\ Sic} : \varepsilon_{\Delta t})$ ....**(13)**

$L(0,i) = [\Delta Em^{\ -1} - p^o - p(i)]^{-1} - (\Delta Em^{\ -1} - p^o)^{-1}$............................**(14)**

$P_{ijkl}(i) = \int \Gamma_{ijkl}(i')di'$............................**(15)**

As the temperature rises the matrix material starts melting and starts forming a viscous fluid where the embedded particulate start to lose cohesion and deboned from the matrix[26]. If coefficient of momentum exchange at Al-SiC interface due to drag created due to strain against dissipative stress is assumed as 'CME' then the value of such drag at all possible interfaces needs to be evaluated. In case of PRMMCs during FSW three interfaces can be identified namely between, solid Al and viscous Al or solid-liquid, viscous Al and Sic particle or liquid-particle and SiC particle and Solid Al or particle solid. Then CME_{lp}, CMEls , can be derived as

$CME_{lp} = \frac{3}{4} \times \frac{P_{vf}}{d_p} \times \frac{L_{vf}\rho_L C_D}{f(h)} |Vp - V_L|$............................**(16)**

P_{vf} is particle volume fraction, d_p is diameter of particle.

L_{vf} is liquid volume fraction, ρ_L is density at given temperature.

$|Vp - V_L|$ is relative velocity, C_D is calculated using stokes law for creeping flow (Re_p<.l)

$C_D = 24/Re_p$

Re_p is Reynold's number of particle.

$Re_p = \frac{\rho_L d_p |Vp - V_L|}{\mu_L}$............................**(17)**

μ_L is dynamic viscosity of Al at given temperature. f(h) is settling function hindrance caused due to multiple particles interaction on relative velocity.

$f(h_L) = \frac{L_{vf}(Vp - V_L)}{V_\infty}$............................**(18)**

V_∞ is called stokes settling velocity for a single particle.

$V_\infty = \frac{{d_p}^2(\rho_L - \rho_P)g}{18\mu_L}$............................**(19)**

ρ_P is particle density, hence

$CME_{LP} = \frac{18\mu_L {L_{vf}}^2 {P_{vf}}^2}{{d_p}^2 f(h_L)}$............................**(20)**

Similarly for CME_{LS} in analogous to Darey law using permeability K_{LS}

$CME_{LS} = \frac{\mu_L {L_{vf}}^2}{K_{Ls}}$............................**(21)**

Where K_{LS} is function of volume fraction, solidification pattern (i.e, equiaxial or columnar) and microstructure.

Using kozney-carman theory$K_{LS} = \frac{K_0 {L_{vf}}^3}{{S_{vf}}^2}$

Both L_{vf} and S_{vf} are for Al and K_0 is experimentally calculated. CME_{ps} is often assumed to be infinity or zero as particle and solid are relatively stationary locally.

$$CME_{ps} = \infty \text{ if } S_{vf} \;\&\; P_{vf} > 0$$

$$= 0 \text{ if } S_{vf} \text{ or } P_{vf} = 0$$............................**(22)**

This is due to as v_p approaches zero at solid interface locally it gets pulled into the viscous liquid due to rotation of the tool and also the solid dendrite micro size is larger when compared to nano scale particulate used in general.

There are scenarios where in the hard particulate gets stuck into soft matrix due to speed of the tool resulting in clustering of particles then if d_c is diameter of such a cluster then $d_c > d_p$ and it traps and drags small volume of liquid along[27]. Under such case resultant volume fraction is

$\left(\frac{P_{vf}}{C_{vf}}\right) + (1 - \frac{P_{vf}}{C_{vf}})C_{vf}$............................**(23)**

2.2 Deep Learning Model

A meso scale 6×6 random stiffness tensor $V_k = \sigma V_k \varepsilon (V_k)^T$ ....**(24)**

σ is a row vector and ε^T is a column vector

V_k where K=1,2,3,….n

Denotes vector in n random dimensions of random space R_s denoting the matrix and particulate when the material RVE is subjected to stress with constant strain at all it boundaries.

Then elastic tensor is given by $el_i^+((x_1, x_2, x_3) - el_i^-((x_1, x_2, x_3) = a\varepsilon_{ij0}$

Where $-a \leq x_i \leq +a$ and el_i^+, el_i^- are values at x_i=+a and x_i=-a respectively[28]. If RVE volume is V then

$\frac{1}{V}\int_{Rs}\int_{v} \varepsilon_{ij}\ (x_1, x_2, x_3 v_R) dv dv_R = \varepsilon_{ij_0}$............................**(25)**

If el_q represents elastic parameters $i.e$ $el_q = [E11, E22, G12]q$. for q=1, 2, 3, 4,…n.

Then deep learning model approximate inputs and outputs using

$el^{\wedge(v_k, w)} = f\left(\sum_{j=1}^{m} w_j\, \varphi_j(v_j)\right) = f(w^T \varphi v_K)$ ....**(26)**

$w^T = w_0, w_1, \ldots w_m$

Are adapted unknown weights for each layer of hidden artificial neural network. Where in φ represents nonlinear orthogonal functions set and f is identity function used for estimation. The w value is initially adapted and f is adjusted while calculating 'w' using φ. The cost function is defined using least squares of parametric estimation [29,30]

$$Arg\ min||l_2(w)|| = \frac{1}{2}\sum_{i=1}^{n} \left[w^T\varphi(C_i) - el_i\right]^2 + \frac{\lambda}{2}||w||^2 \ldots\ldots\ldots\ldots\ldots\ldots\ldots\ldots\ldots (27)$$

Arg min$||l_2(w)||=1/2\ {}^n\sum_{i=1} [w^T\ \varphi(c_i)\text{-}el_i]^2 + \lambda/2\ ||w||^2$

λ is for regularization using over fitting to avoid values reaching large numbers

During training the model aims to minimize cost function. It estimates w and descent it after each iteration k

$$W^{(k+1)} = W^K - \eta^{(K)}\nabla l_2^{(k)}(W) \ldots\ldots\ldots\ldots\ldots\ldots\ldots\ldots\ldots (28)$$

η is step size also called learning rate.$\nabla l_2^{(k)}(W)$ is used to determine descent direction in order to converge cost function to local minimum. The descent gradient can be given by

$$\nabla l_2^{(k)}(W) = \tau^{(k)}(w)^{\tau}\,\theta \ldots\ldots\ldots\ldots\ldots\ldots\ldots\ldots\ldots (29)$$

Where

τ is Jacobian matrix of derivative of network errors with respect to weight calculated using back propagation and θ is network error vector.

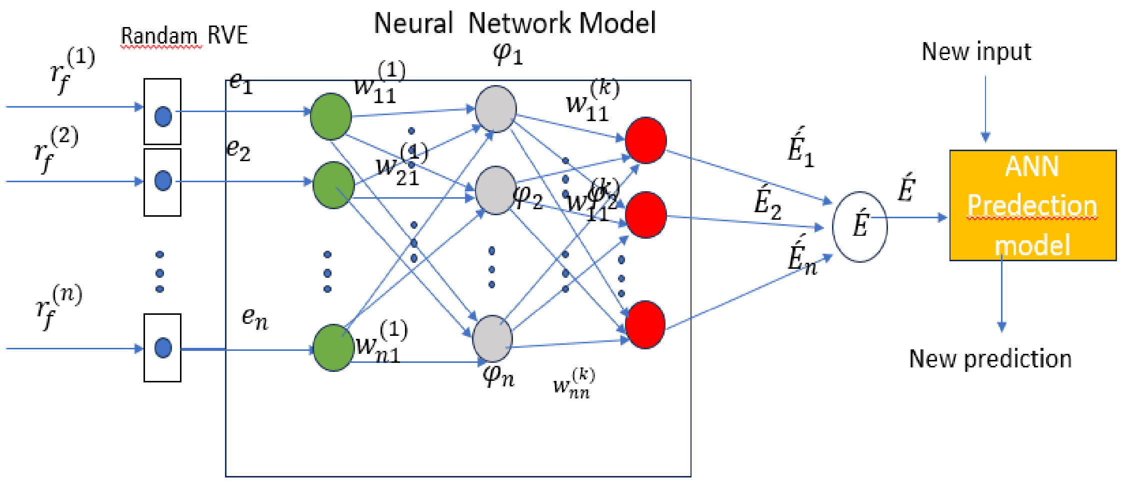

Figure 1. Deep learning model for the prediction

3.Numerical Simulation And Validation

3.1 Numerical Simulation

The above theoretical micro-mechanical model was used to simulate molecular dynamics of PRMMCs during FSW using custom code of C++ which was processed using LAMMPS (Large-scale Atomic/Molecular Massively Parallel Simulator). The resultant simulation was found to be resource hungry thus effecting the accuracy. In order to simplify the processing, a ANN model was introduced to identify the hidden patterns using generalized polynomial chaos model.

Property	Al [matrix]	SiC[particulate]
Elastic modulus	72.1	431

Shear modulus	26.9	181.1
Poissons ratio	0.34	0.19
Coefficient of thermal expansion [10^{-6}/K]	23.6	8.6

Table 1. Material Constant

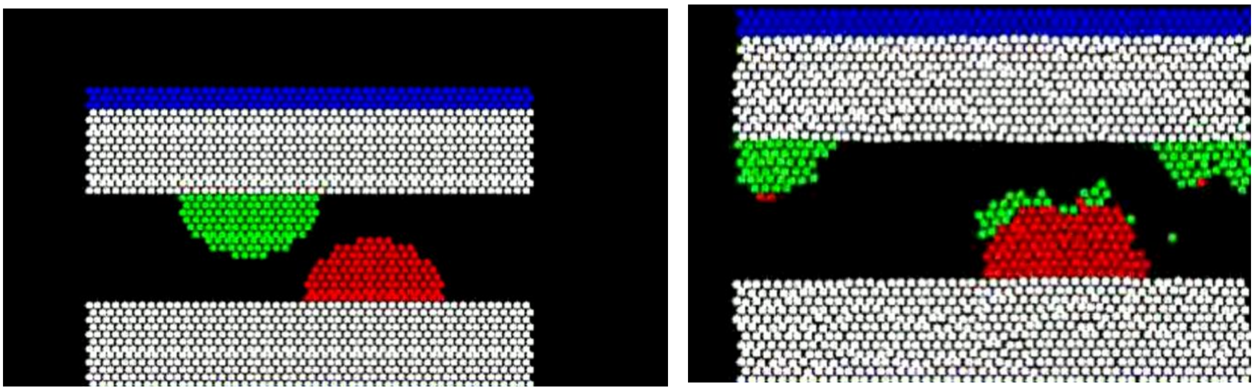

Figure 2. LAMMPS Simulation

A modified micro-mechanical model approximated using deep learning to predict the thermo-mechanical behavior of particulate reinforced metal matrix composite during friction stir welding process was tested. Initially LAMMPS based simulation was used to estimate the material behavior and the results were found to be in alignment with the published literature. The molecular dynamics study required large computational resources and took about 81 hours to estimate the RVE deformations. This was further tweaked using generalized polynomial chaos model to simplify the simulation. Initially the microstructures from different literature were used to train the model and predict a RVE configuration. This approach helped in limiting the RVE permutations. Following which the LAMMPS was used to predict the changes in thermo-mechanical properties of the matrix – particulate interface in form of temperature gradient distribution during FSW along the selected set RVEs

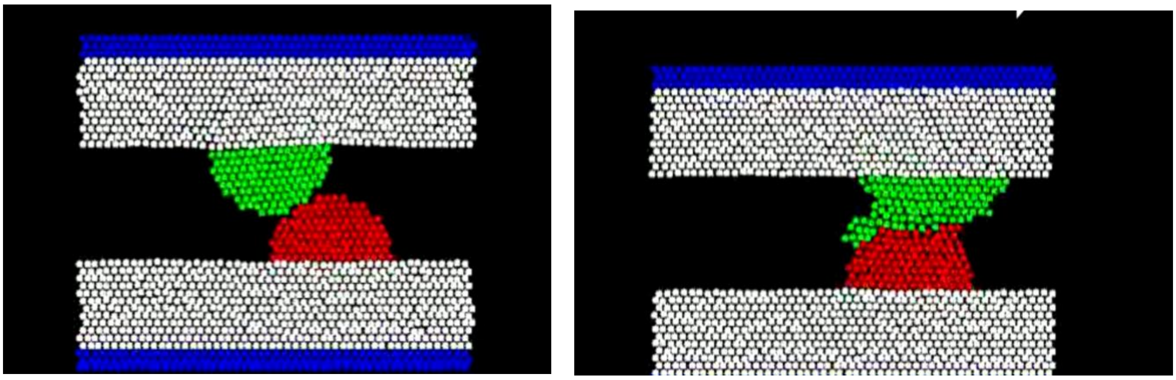

Figure 3. Matrix-Particle interaction during FSW

3.2.Validation

RVEs were extrapolated and validated using an published article by Omar S Salih and H Ou (2019), where in the effects of tool rotation and transverse speed rates on friction stir welded Al-SiC MMC joints was studied and

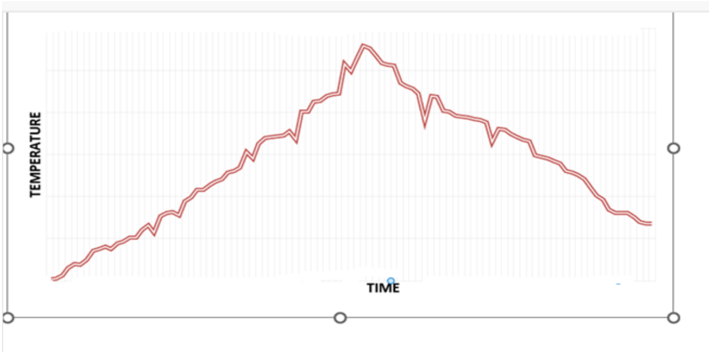

presented. During their experimentation, the authors presented rate of temperature raise and thermal history during tool pass in nugget zone. It was found to be similar to results generated during thermo-mechanical simulation using the numerical model presented and found to validate it.

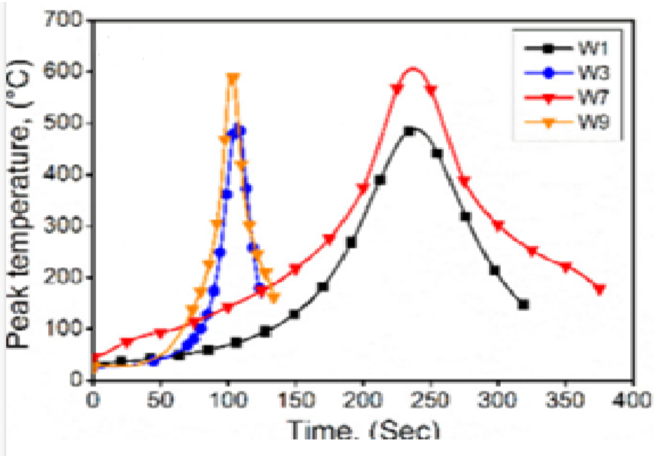

(a) (b)

Validation

(a) From reference (b)Simulated result

RPM	1500
Speed	25mm/min
Density	7800 kg/m^3
Specific heat	460 j/kg/K

Table 2. Tool parameter

During the validation process, the rate of thermal conductivity was calculated using a combination of Maxwell, Brugheman, Hamilton and Crosser models discussed in S.M. Thahab (2016) work.

Reference	**Correlation**	**Conditions**
Maxwell's	$K_{nf} = K_f + 3\varphi \frac{K_P - K_f}{2K_f + K_P} K_f$	Spherical, low volume fractions, random distributed particles

Hamilton and Crosser	$K_{nf} = \frac{K_P + (n-1)K_P - (n-1)(K_P - K_f)\varphi}{K_P + (n-1)K_f + (K_P - K_f)\varphi}$	Spherical, low volume fractions, random distributed particles, for non-spherical n=6
Bruggeman	$K_{nf} = \varphi\left(\frac{K_P - K_{nf}}{(K_P + 2K_{nf})}\right) + (1 - \varphi\left(\frac{K_f - K_{nf}}{(K_f + 2K_{nf})}\right)$	Binary mixture, homogeneous, no limitations on the concentration, random distributed particles

Effective Thermal Conductivity Correlations for Nanofluids is

$K = -1X10^{-8}T^3 + 2X10^{-5}T^2 - 0.0068T + 25.333$ **………………………..(31)**

4. Conclusions

A simplified set of micro mechanical equations driven by deep learning artificial neural network to represent Sic particulate reinforced Al metal matrix composite was developed. Such an approach is found to be effective in conducting in situ studies of molecular dynamics of PRMMC's. Further the thermal rheological behavior during friction stir welding was studied with focus of matrix-particle interaction by simulating the material flow and temperature distribution in visco elastic state. The method is found to be numerically sound and is validated.

References

[1] Kwon, SC; Adachi, T; Araki, W; Yamaji, A. 2008. Effect of composing particles of two sizes on mechanical properties of spherical silica-particulate-reinforced epoxy composites. Composites Part B: Engineering, Volume 39, Issue 4, Pages 740-746

[2] Johan Verbeek. 2003.The Influence of Interfacial Adhesion, Particle Size and Size Distribution on the Predicted Mechanical Properties of Particulate Thermoplastic Composites. Materials Letters 57(13-14):1919-1924

[3] Long-Cheng Tang, Hui Zhang, Stephan Sprenger, Lin ye. 2012. Fracture mechanisms of epoxy-based ternary composites filled with rigid-soft particles. Composites Science and Technology 72(5):558–565

[4] Cho, J., Joshi, M.S., Sun, C.T., 2006. Effects of inclusion size of mechanical properties of polymeric composites with micro and nano
particles. Compos. Sci. Technol. 66, 1941–1952.

[5] Brune, DA., Bicerano, J., 2002. Micromechanics of nanocomposites: comparison of tensile and compressive elastic moduli,
and prediction of effects of incomplete exfoliation and imperfect alignment on modulus. Polymer 43, 369–387.

[6] Chawla, N., Ganesh, V.V., Wunsch, B., 2004. Three-dimensional (3D) microstructure visualization and finite element modeling of the
mechanical behavior of the SiC particle reinforced aluminum composites. Scripta Materialia 51, 161–165.

[7] Kari, S., Berger, H., Rodriguez-Ramos, R., Gabbert, U., 2007. Computational evaluation of effective material properties of composites
reinforced by randomly distributed spherical particles. Compos. Struct. 77, 223–231.

[8] H.L. Duan, X. Yi, Z.P. Huang, J. Wang, 2007, A unified scheme for prediction of effective moduli of multiphase composites with interface effects. Part I: Theoretical framework. Mechanics of Materials 39

94–103

[9] Anastasia Muliana, Kamran A. Khan ,2008, A time-integration algorithm for thermo-rheologically complex polymers, Computational Materials Science, Volume 41, Issue 4, Pages 576-588

[10] Eroshkin, O., Tsukrov, I., 2005. On micromechanical modeling of particulate composites with inclusions of various shapes. International Journal of Solids and Structures, Volume 42, Issue 2, Pages 409-427

[11] W.Xu, Fan Wu, Yang Jiao, Mingjun Lui ,2017,A general micromechanical framework of effective moduli for the design of nonspherical nano- and micro-particle reinforced composites with interface properties, Materials & Design Volume 127, Pages 162-172

[12] Ju, J.W., Chen, T.M., 1994. Elastic moduli of the two phase composites containing randomly dispersed spherical inhomogeneities. Acta Mech. 103, 123–144.

[13] Luo, J.J., Daniel, I.M., 2003. Characterization and modeling of mechanical behavior of polymer/clay nanocomposites. Compos. Sci. Technol. 63 (11), 1607–1616.

[14] Ma, H., Hu, G., Huang, Z., 2004. A micromechanical method for particulate composites with finite particle concentration. Mech. Mater. 36, 359–368

[15] Odegard, G.M., Clancy, T.C., Gates, T.S., 2005. Modeling of the mechanical properties of nanoparticle/polymer composites. Polymer 46, 553–562.

[16] Zheng, Q.S., Du, D.X., 2001. An explicit and universally applicable estimate for the effective properties of multiphase composite which accounts for inclusion distribution. J. Mech. Phys. Solids 49 (11), 2765–2788.

[17] Sheng, N., Boyce, M.C., Parks, D.M., Rutledge, G.C., Abes, J.I.,Cohen, R.E., 2004. Multiscale micromechanical modeling of polymer/clay nanocomposites and the effective clay particle. Polymer 45, 487–506.

[18] Peng, X.; Hu, N.; Zheng, H.; Fukunaga, H. Evaluation of mechanical properties of particulate composites with a combined self-consistent and Mori-Tanaka approach. Mech. Mater. 2009, 41, 1288–1297.

[19] Raju, B.; Hiremath, S.R.; Mahapatra, D.R. A review of micromechanics based models for effective elastic properties of reinforced polymer matrix composites. Compos. Struct. 2018, 204, 607–619.

[20] Roh, Y.; Heo, G.; .; Whang, S. A Survey on Data Collection for Machine Learning: A Big Data—AI Integration Perspective. IEEE Trans. Knowl. Data Eng. 2019, 1, 1–20.

[21] Chen, C.T.; Gu, G. Machine learning for composite materials. MRS Commun. 2019, 9, 556–566

[22] Sacco, C.; Baz Radwan, A.; Anderson, A.; Harik, R.; Gregory, E. Machine learning in composites manufacturing: A case study of Automated Fiber Placement inspection. Compos. Struct. 2020, 250, 112514.

[23] Peter McCullagh, 2018, Tensor Methods in Statistics, Dover Publications, New York

[24] Pavel Grinfeld, 2013, Introduction to Tensor Analysis and the Calculus of Moving Surface, Springer New York, NY

[25] A. Abdelfattah, M. Baboulin,V.Dobrev, J. Dongarra,C.Earl,J. Falcou, A. Haidar, I. Karlin, Tz. Kolev, I. Masliah and S. Tomov, 2016, High-Performance Tensor Contractions for GPUs, The International Conference on ComputationalScienc, Procedia Computer Science, Volume 80, Pages 108–118.

[26] . Kun Zhou, 2012, Elastic field and effective moduli of periodic composites with arbitrary inhomogeneity distribution, Acta Mechanica, Volume 223, pages 293–308

[27] Jacob Aboudi, 2013. Mechanics of composite materials: a unified micromechanical approach. Elsevier.

[28] Heinbockel, J. H. 2002. Introduction to tensor calculus and continuum mechanics. Trafford. Victoria.29. Amir Kordijazi, Tian Zhao, Jun Zhang, Khaled Alrfou & Pradeep Rohatgi ,

[29] 2021, A Review of Application of Machine Learning in Design, Synthesis, and Characterization of Metal Matrix Composites: Current Status and Emerging Applications, Machine Learning in Design, Synthesis, and Characterization of Composite Materials, Volume 73, pages 2060–2074

[30] , Jessica Karaguesian, Jaclyn R. Lunger, Aik Rui Tan, Mingrou Xie, Jiayu Peng, and Rafael Gómez-Bombarelli, 2023, Representations of Materials for Machine Learning, Annual Review of Materials Research 53:1, 399-426